

# On the Bioactivity and Mechanical Properties of Gehlenite Nanobioceramic: A Comparative Study

## Abstract

**Background:** For a new biomaterial which is going to be applied in bone tissue regeneration, bioactivity (bone bonding ability) and desirable mechanical properties are very essential parameters to take into consideration. In the present study, the gehlenite's mechanical properties and bioactivity are assessed and compared with hydroxyapatite (HA) for bone tissue regeneration. **Method:** Gehlenite and HA nanoparticles are synthesized through sol-gel method and coprecipitation technique, respectively, and their physical and chemical properties are characterized through X-ray diffraction, Fourier transform infrared spectroscopy, and transmission electron microscopy. **Results:** The results prove that the gehlenite and HA phases without any undesirable phase are obtained, and the particles of both compounds are in the nanometer range with spherical morphology. The compressive strength of both compounds are assessed, and the values for gehlenite and HA disks are  $144 \pm 5$  and  $150 \pm 4.8$  MPa, respectively. Next, their bioactivity potential is assessed into simulated body fluid (SBF) up to 21 days, and the results show that after 14 days, gehlenite disk's surface is completely covered with newly formed Ca-P particles. However, some sporadic precipitations after 21 days soaking into SBF are formed onto the HA disk's surface. **Conclusion:** This comparative study shows that nanostructured gehlenite disk with desirable mechanical properties and faster bioactivity kinetic than HA can be considered as a promising bioceramic for bone tissue regeneration.

**Keywords:** Bioactivity, gehlenite, hydroxyapatite, mechanical properties

Submitted: 19-Aug-2019

Revised: 12-Oct-2019

Accepted: 30-Jan-2020

Published: 25-Apr-2020

## Introduction

It is well known that bone tissue as a composite contains organic and inorganic phases which are mainly collagen and hydroxyapatite (HA,  $\text{Ca}_{10}(\text{PO}_4)_6\text{OH}_2$ ), respectively. Based on the existence of calcium phosphate into the bone's structure, calcium phosphate-based bioceramics (CPBs) including HA and  $\beta$ -tricalcium phosphate are of particular interest for different kinds of purposes among which bone substitution and regeneration can be enumerated.<sup>[1,2]</sup> It is important to note that calcium CPBs have good biocompatibility and their chemical composition similarity to host bone would assure their bonding to the bone (bioactivity). However, two inevitable issues should be considered; first, CPBs specifically HA suffer from weak mechanical properties and to compensate

that sintering in high temperatures is required resulting in turning HA to nonbiodegradable material susceptible to long term failure; second, the kinetic of triggering biological carbonated HA on the bone substitute is another important issue which has attracted lots of attention. Therefore, a bone substitute with faster bioactivity potential is more desirable than the one which needs for instance 1 month to be coated with carbonated HA. It should be mentioned that sintered HA suffers from forming carbonated HA on its surface in a few days.<sup>[3-5]</sup>

Through past three decades, calcium-containing silicate-based bioceramics (CSBs) including bioactive glass and glass-ceramics have attracted lots of attention for bone tissue regeneration rooting in stimulatory and therapeutic effects of calcium and silicon ions on osteoblasts' proliferation, differentiation, and mineralization.<sup>[6]</sup> Calcium silicate with

Ashkan Bigham<sup>1</sup>,  
Saeed Kermani<sup>2,3</sup>,  
Ahmad Saudi<sup>4</sup>,  
Amir Hamed  
Aghajanian<sup>5</sup>,  
Mohammad  
Rafienia<sup>6</sup>

<sup>1</sup>Department of Materials Engineering, Advanced Materials Research Center, Najafabad Branch, Islamic Azad University, Najafabad, <sup>2</sup>Department of Bioelectronics and Biomedical Engineering, School of Advanced Technologies in Medicine, Isfahan University of Medical Sciences, <sup>3</sup>Medical Image and Signal Processing Research Center, Isfahan University of Medical Sciences, <sup>4</sup>Student Research Committee, School of Advanced Medical Technologies in Medicine, Isfahan University of Medical Sciences, Isfahan, <sup>5</sup>Department of Materials Engineering, Faculty of Engineering, Razi University, Kermanshah, <sup>6</sup>Biosensor Research Center, Isfahan University of Medical Sciences, Isfahan, Iran

**Address for correspondence:**  
Dr. Saeed Kermani,  
Department of Bioelectronics and Biomedical Engineering, School of Advanced Technologies in Medicine, Isfahan University of Medical Sciences, Isfahan, Iran.  
E-mail: kermani@med.mui.ac.ir

Access this article online

Website: [www.jmssjournal.net](http://www.jmssjournal.net)

DOI: 10.4103/jmss.JMSS\_41\_19

Quick Response Code:



**How to cite this article:** Bigham A, Kermani S, Saudi A, Aghajanian AH, Rafienia M. On the bioactivity and mechanical properties of gehlenite nanobioceramic: A comparative study. *J Med Signals Sens* 2020;10:105-12.

This is an open access journal, and articles are distributed under the terms of the Creative Commons Attribution-NonCommercial-ShareAlike 4.0 License, which allows others to remix, tweak, and build upon the work non-commercially, as long as appropriate credit is given and the new creations are licensed under the identical terms.

For reprints contact: [reprints@medknow.com](mailto:reprints@medknow.com)

CaSiO<sub>3</sub> chemical formula belongs to the CSBs family, and it has been applied in bone tissue regeneration widely because of its better bioactivity than traditional CPBs.<sup>[7]</sup> However, there is a significant disadvantage for CaSiO<sub>3</sub> ceramic which is its high dissolution rate resulting in high pH increase in the surrounding medium and it subsequently leads to cytotoxicity due to alkalinity.<sup>[8]</sup> It has been suggested that incorporation of different elements into CaSiO<sub>3</sub> would highly affect its physical, chemical, and biological properties. These elements including magnesium, zinc, strontium, aluminum, titanium, and zirconium are able to provide CaSiO<sub>3</sub> more stable dissolution rate, better mechanical properties, bioactivity, and cell compatibility.<sup>[9]</sup> Gehlenite with Ca<sub>2</sub>Al<sub>2</sub>SiO<sub>7</sub> chemical formula is composed of CaO, Al<sub>2</sub>O<sub>3</sub>, and SiO<sub>2</sub>, and it recently found its way in bone tissue engineering. In 2016, gehlenite for the first time is introduced as a promising bioceramic with great mechanical properties supporting human osteoblast cells attachment and proliferation for bone tissue regeneration.<sup>[10]</sup> In our previous study in 2018, gehlenite nanoparticles were synthesized through sol-gel method for the first time.<sup>[11]</sup> It is important to notice that gehlenite is still in its primitive stages to be considered for bone tissue regeneration applications and more studies are required to discover its potentials and drawbacks.

In the present study, gehlenite nanoparticles are synthesized through sol-gel method in acidic medium and for better understanding about its physical and chemical properties, HA as a gold standard material for bone tissue regeneration is also synthesized via co-precipitation technique and the bioactivity potential and mechanical properties of these materials are compared *in vitro*.

## Materials and Methods

### Synthesis of gehlenite nanopowder

As it is mentioned before, sol-gel method in acidic medium is used for synthesis of gehlenite nanopowder, and the precursors are as follows: tetraethyl orthosilicate ([C<sub>2</sub>H<sub>5</sub>O]<sub>4</sub>Si, TEOS), aluminum nitrate nonahydrate (Al[NO<sub>3</sub>]<sub>3</sub>·9H<sub>2</sub>O), and calcium nitrate tetrahydrate (Ca[NO<sub>3</sub>]<sub>2</sub>·4H<sub>2</sub>O) (all from Merck, Germany). In the first step, TEOS is added to the mixture of deionized water and 2M HNO<sub>3</sub> solution to be hydrolyzed followed by preserving the solution in this condition for 30 min under vigorous stirring (TEOS/H<sub>2</sub>O/HNO<sub>3</sub> = 1:8:0.16). Next, the nitrate-based precursors including Ca(NO<sub>3</sub>)<sub>2</sub>·4H<sub>2</sub>O and Al(NO<sub>3</sub>)<sub>3</sub>·9H<sub>2</sub>O are added into the mixture one after another for further reaction based on the molar ratio of Ca, Al, and Si in gehlenite formula. The vigorous stirring is kept for further 5 h at room temperature, and eventually, the mixture is statically preserved for aging at 60°C for 24 h to form wet gel and then dried at 120°C for 48 h. The final dried gel is ground, sieved, and calcined at 1300°C with 10°C min<sup>-1</sup> heat rate for 3 h. The gehlenite powder after heat treatment is exposed to ball milling process by

which the agglomeration could be removed and the powder becomes more homogenous. The parameters of ball milling are as follows: the ratio of ball/powder is set on 10/1, time: 8 h, and rotational speed: 250 rpm.

### Synthesis of hydroxyapatite nanopowder

To synthesize the HA nanopowder co-precipitation technique is applied and to get this done, calcium chloride (CaCl<sub>2</sub>, Merck, Germany) and trisodium phosphate dodecahydrate (Na<sub>3</sub>PO<sub>4</sub>·12H<sub>2</sub>O, Merck, Germany) are used. First, two separate solutions for CaCl<sub>2</sub> and Na<sub>3</sub>PO<sub>4</sub>·12H<sub>2</sub>O are provided and it should be mentioned that the chloride solution temperature is kept at 45°C, whereas the phosphate solution's temperature is set at 95°C. Second, the chloride solution is then added dropwise to the phosphate solution under continuous stirring. Finally, the precipitates are filtered, rinsed, and dried for 24 h followed by calcination at 900°C with 10°C min<sup>-1</sup> heat rate for 3 h. It should be noticed that the molar ratio of Ca<sup>2+</sup> to PO<sub>4</sub><sup>-3</sup> is 1.67 to obtain HA nanopowder.

### Preparation of gehlenite and hydroxyapatite disks

In the case of bioactivity and mechanical properties assessment, gehlenite and HA nanoparticles are used to fabricate disks (*d* = 30 mm and *h* = 15 mm) as follows: The calcined powders are uniaxially pressed at 300 MPa, and then, the disks are exposed to heat treatment for sintering at 1000°C for 3 h in an electric furnace. The heating rate is set on 5°C/min.

### Characterization

The physical and chemical properties of gehlenite and HA nanoparticles are assessed through X-ray diffraction (XRD, Philips TW3710, Netherlands) for structural analyses, transmission electron microscopy (TEM, JEM-100CX, Japan) and field-emission scanning electron microscopy (FESEM, SU3500, Hitachi, Japan) equipped with energy dispersive spectroscopy (EDS) for microstructural and elemental analyses, Fourier transform infrared spectroscopy (FTIR, Spectrume GX, USA) for chemical bonds and surface groups assessment, and atomic force microscopy (AFM, Ara-AFM-model number 0101/A, Iran) for surface roughness assessment.

The compressive strength of gehlenite and HA disks are measured through a computer controlled universal testing machine (Instron Wolpert, Darmstadt, Germany) with a crosshead speed of 0.5 mm min<sup>-1</sup> based on ASTM C1323-16, and it is noteworthy that three similar disks are used and the results are based on mean ± standard deviation (SD).

### Bioactivity

The bioactivity test is carried out through immersion of the disks into simulated body fluid (SBF) up to 21 days *in vitro* and the disks at each time period are removed

from the SBF, rinsed with distilled water and dried into an oven at 60°C for 24 h. The surface of each disk relating to gehlenite and HA are assessed after immersion into SBF using FESEM equipped with EDS to observe the surfaces and detect the elements of newly formed precipitations. It should be noticed that the ions concentrations are measured for each disk up to 21 days by inductively coupled plasma (ICP, Varian BV ES-700, Australia) and the pH variations and ICP results are based on mean  $\pm$  SD of three disks.

The Kokubo's protocol is used to prepare SBF.<sup>[12]</sup> The volume of SBF for each disk is calculated by Eq. 1:

$$V_s = \frac{S_a}{10} \quad (1)$$

Where  $S_a$  is the surface area of the scaffold (mm<sup>2</sup>) and  $V_s$  is the SBF volume (mL).

## Results and Discussion

### Characterization of hydroxyapatite nanoparticles

The results relating to characterization of HA nanoparticles including XRD, FTIR, and TEM are provided in Figure 1. Figure 1a indicates the XRD pattern of HA, and besides, the Joint Committee on Powder Diffraction Standards (JCPDS) pattern of HA (01-084-1997) as a reference is shown below the HA XRD pattern which is synthesized in the present study. Through taking a glance on the XRD patterns, it can be deduced that the HA pattern is highly in good agreement with the JCPDS pattern proving successful crystallization of the HA at 900°C. The FTIR spectrum of HA is exhibited through Figure 1b and the reason why this test is taken roots in discovering the surface chemical groups. There are six bands visible including 636, 717, 964, 1021, 1088, and 1654 cm<sup>-1</sup> in the FTIR spectrum. The two bands at 636

and 717 cm<sup>-1</sup> are attributed to the phosphate bending mode and the bands at 964, 1021, and 1088 cm<sup>-1</sup> are related to the phosphate stretching modes.<sup>[13,14]</sup> The existence of band at 1654 cm<sup>-1</sup> confirms the bending mode of water which is absorbed on the surface of HA.<sup>[15]</sup> The microstructural properties of the calcined HA are shown through TEM micrographs [Figure 1c and d]. Two TEM micrographs with different magnifications are provided, and it is visible that the HA particles have a size <100 nm and their morphology is almost spherical, and it should be mentioned that due to high surface energy of nanoparticles, they have a great tendency to become agglomerated [Figure 1].<sup>[16]</sup>

### Characterization of gehlenite nanoparticles

The same characterization techniques, which are done for HA nanoparticles, are carried out for Gehlenite nanoparticles and they are indicated through Figure 2, where Figure 2a shows the XRD pattern of gehlenite nanoparticles and the crystal planes of calcined gehlenite nanoparticles are in a great agreement with the JCPDS pattern of gehlenite (01-079-2421) proving successful synthesis strategy. Figure 2b exhibits the FTIR pattern of gehlenite nanoparticles in which seven distinguishable bands are observable. The bands including 642, 711, 802, 848, 968, 1107, and 3010 cm<sup>-1</sup> represent metal-oxygen vibrations (Ca–O–Ca), symmetric stretching vibrations from Si–O bands, Si–O–Al, Al–O vibrations (848 and 968 cm<sup>-1</sup>), asymmetric stretching vibrations of Si–O–Si, and stretching vibrations of OH groups due to water absorption, respectively.<sup>[17,18]</sup> Figure 2c and d indicates the morphology and particle size of gehlenite nanoparticles with two magnifications. The TEM micrographs clearly show that a narrow distribution exists among the particles size, and also, the nanoparticles with spherical morphology are homogeneously distributed [Figure 2].

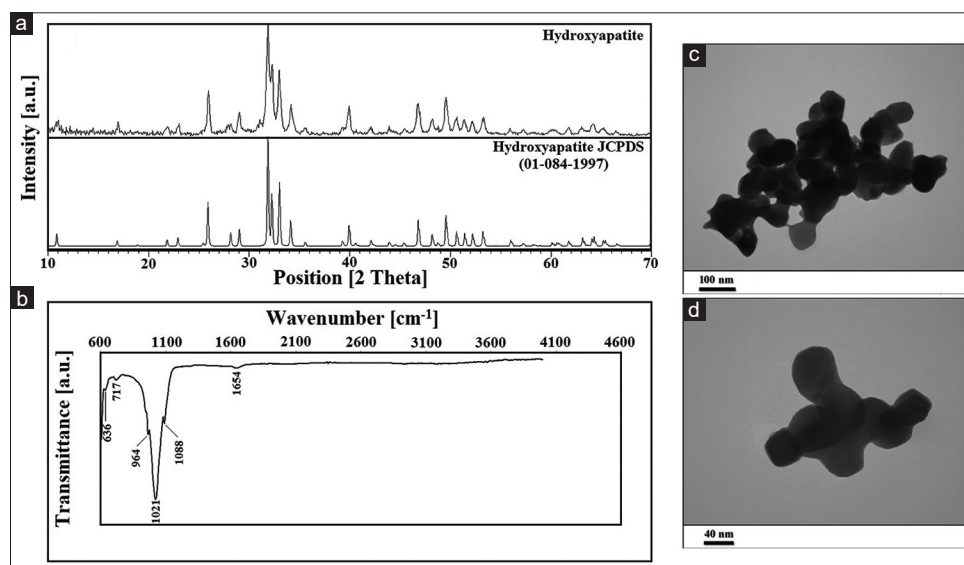


Figure 1: X-ray diffraction pattern (a), Fourier transform infrared spectroscopy pattern (b), and TEM micrographs of hydroxyapatite nanoparticles (c and d)



### Characterization of hydroxyapatite and gehlenite disks

The geometrical properties (topography and roughness) and elemental analyses of HA and gehlenite disks, which are sintered at 1000°C, are exhibited in Figure 3. Figure 3a-c shows the surface image, amounts of roughness, and elemental analysis of HA disk. Through Figure 3a, it is clear that there are some pits on the surface of HA disk. Through AFM micrograph [Figure 3b], it also can be seen the surface roughness is about 448 nm and the EDS analysis clearly proves that the main elements in the structure of HA including Ca, P, and O are present. It is

noteworthy that the existence Au peaks relates to the process of FESEM imaging. On the other hand, gehlenite's surface has more pits than the surface of HA disk and these pits may be resulted from some the shrinkage during sintering process [Figure 3d].<sup>[19]</sup> The AFM result of gehlenite surface is in agreement with the FESEM micrograph, and EDS analysis indicates that all elements of gehlenite structure such as Ca, Si, Al, and O are present, and there is no impurity detectable. By comparison between both compounds, it can be inferred that the roughness of gehlenite's surface is more than HA's surface, and it

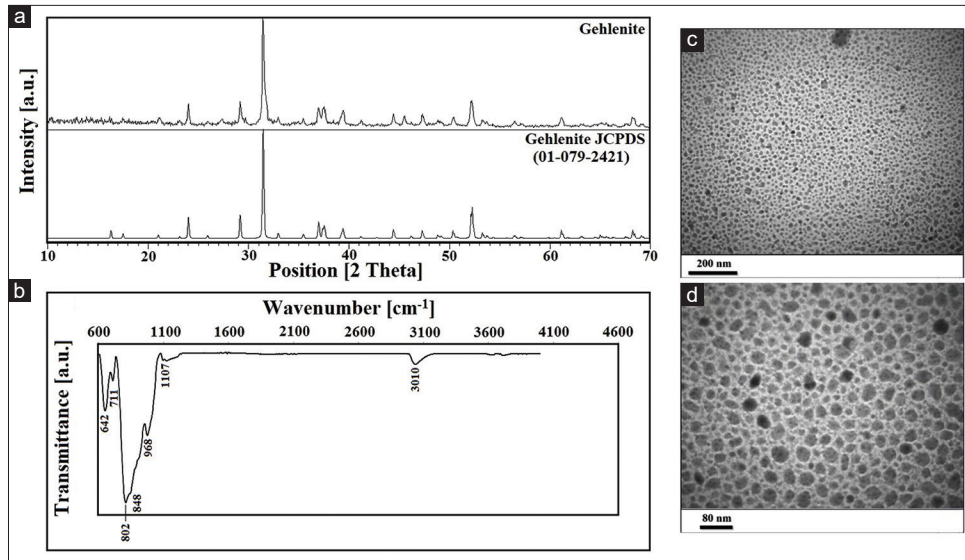


Figure 2: X-ray diffraction pattern (a), Fourier transform infrared spectroscopy pattern (b), and TEM micrographs of gehlenite nanoparticles (c and d)

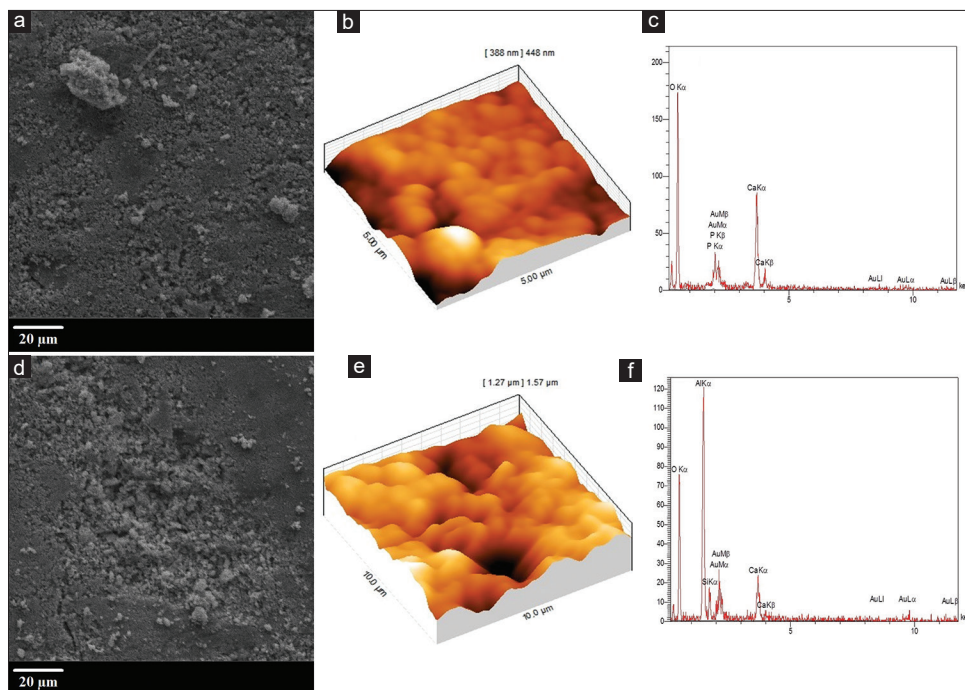


Figure 3: Field-emission scanning electron microscopy and atomic force microscopy micrographs (the area roughness [Sq]), and energy dispersive spectroscopy analyses of hydroxyapatite disk (a-c) and gehlenite disk (d-f)

should be mentioned that the geometrical properties of a material have significant effects on its physical, chemical, and biological properties.<sup>[20]</sup> Nonetheless, the compressive strengths of HA and gehlenite disks are assessed and the results show that  $150 \pm 4.8$  and  $144 \pm 5$  MPa are obtained for HA and gehlenite disks, respectively. These amounts of compressive strengths, which are obtained for both disks, are comparable to cortical bone.<sup>[21]</sup> The reason why less compressive strength is observed for gehlenite disk roots in the sintering temperature;  $1000^\circ\text{C}$  is generally reported to be an appropriate temperature for HA to be sintered; but, in this temperature, complete sintering for gehlenite does not occur. Choosing this sintering temperature stems from reducing the differences in geometrical parameters like topography and roughness for more genuine comparison between both compounds. Moreover, another aim for

sintering gehlenite at this temperature is testing its physical, chemical, and biological properties for possible usage in a particulate form like as a reinforcement phase in electrospun-based scaffolds [Figure 3].

### Bioactivity potential

Bioactivity is regarded as a basic requirement for a biomaterial, which is intended to be in contact with bone tissue, and through formation of carbonated HA on the biomaterial, it can make a strong bond with host bone.<sup>[22]</sup> The bioactivity potential of gehlenite and HA disks into SBF is assessed up to 21 days, and the related results are indicated through Figure 4. Moreover, the ions concentrations including  $\text{Ca}^{2+}$ ,  $\text{SiO}_4^{4-}$ ,  $\text{AlO}_3^{3-}$ , and  $\text{PO}_4^{4-}$ , and pH values during soaking period for both compounds are measured and exhibited in Figure 5. Figure 4 shows

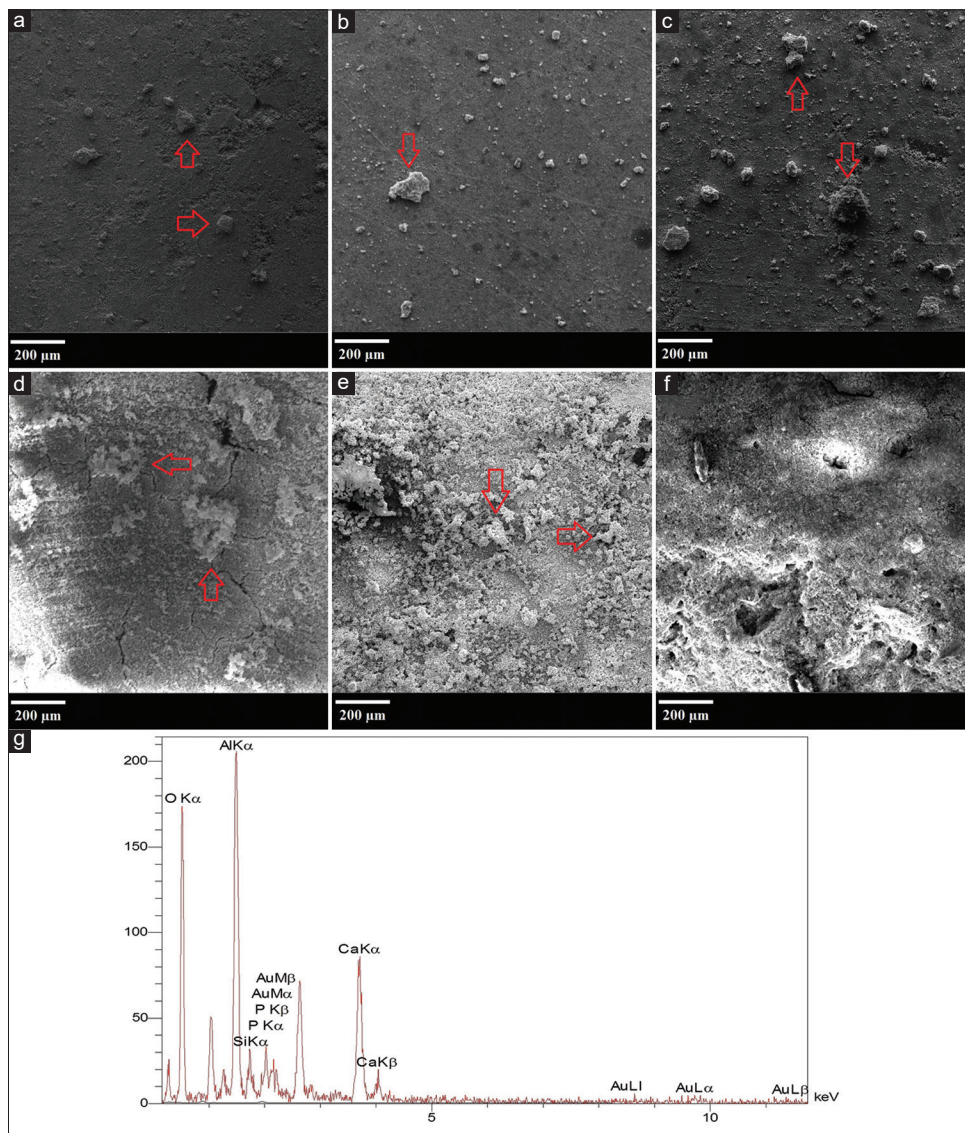


Figure 4: Field-emission scanning electron microscopy micrographs of hydroxyapatite disk after 7 (a), 14 (b), and 21 days soaking into simulated body fluid (c), field-emission scanning electron microscopy micrographs of gehlenite disk after 7 (d),<sup>[11]</sup> 14 (e), and 21 days soaking into simulated body fluid (f), energy dispersive spectroscopy analysis of gehlenite disk after 21 days of soaking into simulated body fluid (g) (newly formed precipitations are shown with red arrows)

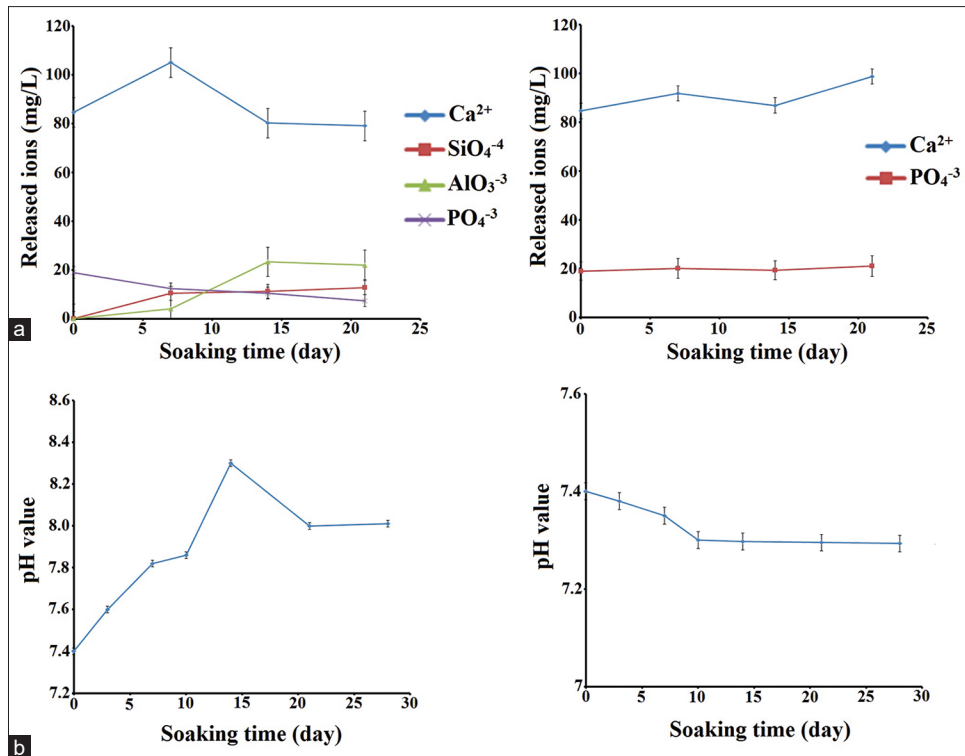


Figure 5: The plots of Ca<sup>2+</sup>, SiO<sub>4</sub><sup>-4</sup>, AlO<sub>3</sub><sup>-3</sup>, and PO<sub>4</sub><sup>-3</sup> ions concentrations (a) and pH variations (b) of gehlenite disks into simulated body fluid,<sup>[10]</sup> The plots of Ca<sup>2+</sup> and PO<sub>4</sub><sup>-3</sup> ions concentrations (c) and pH variations (d) of hydroxyapatite disks into simulated body fluid

the FESEM micrographs of HA [Figure 4a-c] and gehlenite [Figure 4d-f] surfaces after 7, 14, and 21 days immersion into SBF; whereas in the case of HA, it is completely clear that some precipitations are deposited on the surface, but even after 21 days soaking into SBF, the surface is not completely covered with newly formed Ca-P depositions (newly formed precipitations are shown with red arrows). On the other hand, gehlenite's surface seems to be completely covered with newly formed Ca-P particles after 14 days soaking, and after 21 days soaking, the surface precipitations are accumulated and thickened proving higher bioactivity potential of gehlenite than HA (newly formed precipitations are shown with red arrows). In addition, an EDS analysis from gehlenite's surface after 21 days soaking into SBF is taken to determine the elements of surface depositions and it turned out that beside Ca, Si, Al, and O elements which belong to gehlenite structure, P is also detected [Figure 4g]. For better understanding of the bioactivity potential of both compounds, the ions' release trends and pH values are carefully assessed and they are shown in Figure 5. Figure 5a and b exhibits the ions concentrations and pH value of gehlenite disk up to 21 days and 28 days soaking in SBF, respectively. It is observable that Ca<sup>2+</sup> concentration is raised significantly during the first 7 days and then experiences a downward slope up to 14 days and finally becomes steady up to 21 days soaking. However, PO<sub>4</sub><sup>-3</sup> concentration experiences continually decrease up 21 days showing its consuming during soaking period. It is critical to bear in mind that

the raising of Ca<sup>2+</sup> ions concentration during the first 7 days of soaking roots in the dissolution of Ca<sup>2+</sup> ions from the gehlenite's structure; but, between the day of 7<sup>th</sup> and 14<sup>th</sup>, it dramatically decreases proving its consumption in this time period and these results are in a good agreement with the FESEM micrographs [Figure 4d and e] showing that on the day of 14<sup>th</sup>, the surface is totally covered with newly formed depositions.<sup>[9]</sup> The SiO<sub>4</sub><sup>-4</sup> ions show an upward trend up to 7 days followed by a steady state up to 21 days soaking. In the case of AlO<sub>3</sub><sup>-3</sup> ion, it shows a slight increase in its concentration up to 7 days followed by a significant growth in the concentration up to 14 days, and then, it becomes steady. It can be inferred that due to the gehlenite degradation, AlO<sub>3</sub><sup>-3</sup> ions start to be released and then they are consumed when the ions exchange is continued up to 21 days. It is well-known that AlO<sub>3</sub><sup>-3</sup> ions have a tendency to make interaction with PO<sub>4</sub><sup>-3</sup> ions to produce aluminum phosphate and that may be the reason why its concentration is lowered.<sup>[11]</sup> Figure 5b exhibits the pH values of SBF in the exposure of gehlenite disk, where an upward trend is visible up to 14 days (8.3) followed by a downward trend and then a steady state. Releasing Ca<sup>2+</sup> and AlO<sub>3</sub><sup>-3</sup> ions with alkalinity essence is to blame for increasing pH up to 14 days, and their consumption causes the pH to decrease.<sup>[11,23]</sup> The results attributing to HA ion concentrations and pH values are shown in Figure 5c and d in which it can be seen that at each time interval, Ca<sup>2+</sup> liberation goes up and down showing the ion exchange into SBF during the soaking period. It can



be deduced that during the first 7 days, the degradation is dominated and caused increasing in  $\text{Ca}^{2+}$  concentration, and then, these ions are consumed leading to decrease in the concentration.  $\text{PO}_4^{4-}$  ions show a steady release trend with a slight difference. Figure 5d is also indicating that during first 10 days of immersion, a slight decrease in pH occurs followed by steady line up to 28 days.

The whole bioactivity results show that gehlenite disk has higher bioactivity kinetic than HA disk and it may make a strong bond with host bone tissue in earlier days of implantation leading to faster fixation in the bone defect [Figures 4 and 5].

## Conclusion

Gehlenite and HA nanoparticles are synthesized through sol-gel method and co-precipitation technique, respectively, and both of them are carefully characterized through XRD, FTIR, and TEM. The results prove successful crystallization of both compounds without any undesirable phase and they have both exhibited spherical morphology with particle size  $<100$  nm. Moreover, the mechanical properties and bioactivity potential (up to 21 days) of both compounds are assessed and compared with each other. The results of this study show that gehlenite with desirable compressive strength close to cortical bone has better bioactivity potential than HA and it can be considered as a bioceramic with promising potential for bone tissue regeneration.

## Acknowledgment

The authors are thankful for the contributions and supportings of Biosensor Research Center of Isfahan University of Medical Sciences (Grant no. 297171).

## Financial support and sponsorship

None.

## Conflicts of interest

There are no conflicts of interest.

## References

- Foroughi F, Hassanzadeh-Tabrizi SA, Bigham A. *In situ* microemulsion synthesis of hydroxyapatite-MgFe<sub>2</sub>O<sub>4</sub> nanocomposite as a magnetic drug delivery system. *Mater Sci Eng C Mater Biol Appl* 2016;68:774-9.
- Hasegawa K, Turner CH, Burr DB. Contribution of collagen and mineral to the elastic anisotropy of bone. *Calcif Tissue Int* 1994;55:381-6.
- Mondal S, Pal U. 3D hydroxyapatite scaffold for bone regeneration and local drug delivery applications. *J Drug Deliv Sci Technol* 2019;53:101131.
- Bigham A, Aghajanian AH, Behzadzadeh S, Sokhani Z, Shojaei S, Kaviani Y, *et al.* Nanostructured magnetic Mg<sub>2</sub>SiO<sub>4</sub>-CoFe<sub>2</sub>O<sub>4</sub> composite scaffold with multiple capabilities for bone tissue regeneration. *Mater Sci Eng C Mater Biol Appl* 2019;99:83-95.
- Hadidi M, Bigham A, Saebnoori E, Hassanzadeh-Tabrizi SA, Rahmati S, Alizadeh MZ, *et al.* Electrophoretic-deposited hydroxyapatite-copper nanocomposite as an antibacterial coating for biomedical applications. *Surf Coat Technol* 2017;321:171-9.
- Ghadiri S, Hassanzadeh-SA, Bigham A. The effect of synthesis medium on structure and drug delivery behavior of CTAB-assisted sol-gel derived nanoporous calcium-magnesium-silicate. *J Sol-Gel Sci Technol* 2017;83:229-36.
- Lin K, Xia L, Li H, Jiang X, Pan H, Xu Y, *et al.* Enhanced osteoporotic bone regeneration by strontium-substituted calcium silicate bioactive ceramics. *Biomaterials* 2013;34:10028-42.
- Zreiqat H, Ramaswamy Y, Wu C, Paschalidis A, Lu Z, James B, *et al.* The incorporation of strontium and zinc into a calcium-silicon ceramic for bone tissue engineering. *Biomaterials* 2010;31:3175-84.
- No YJ, Li JJ, Zreiqat H. Doped calcium silicate ceramics: A new class of candidates for synthetic bone substitutes. *Materials (Basel)* 2017;10. pii E153.
- Roohani-Esfahani SI, No YJ, Lu Z, Ng PY, Chen Y, Shi J, *et al.* A bioceramic with enhanced osteogenic properties to regulate the function of osteoblastic and osteoclastic cells for bone tissue regeneration. *Biomed Mater* 2016;11:035018.
- Rafienia M, Bigham A, Saudi A, Rahmati S. Gehlenite nanobioceramic: Sol-gel synthesis, characterization, and *in vitro* assessment of its bioactivity. *Mater Lett* 2018;225:89-92.
- Kokubo T, Takadama H. How useful is SBF in predicting *in vivo* bone bioactivity? *Biomaterials* 2006;27:2907-15.
- Foroughi F, Hassanzadeh-SA, Amighian J. Microemulsion synthesis and magnetic properties of hydroxyapatite-encapsulated nano CoFe<sub>2</sub>O<sub>4</sub>. *J Magn Magn Mater* 2015;382:182-7.
- Foroughi F, Hassanzadeh-Tabrizi SA, Amighian J, Saffar-Teluri SS. A designed magnetic CoFe<sub>2</sub>O<sub>4</sub>-hydroxyapatite core-shell nanocomposite for Zn(II) removal with high efficiency. *Ceram Int* 2015;41:6844-50.
- Bigham A, Foroughi F, Motamedi M, Rafienia M. Multifunctional nanoporous magnetic zinc silicate-ZnFe<sub>2</sub>O<sub>4</sub> core-shell composite for bone tissue engineering applications. *Ceram Int* 2018;44:11798-806.
- Bigham A, Saudi A, Rafienia M, Rahmati S, Bakhtiyari H, Salahshouri F, *et al.* Electrophoretically deposited mesoporous magnesium silicate with ordered nanopores as an antibiotic-loaded coating on surface-modified titanium. *Mater Sci Eng C Mater Biol Appl* 2019;96:765-75.
- Khamsehshari N, Hassanzadeh-Tabrizi SA, Bigham A. Effects of strontium adding on the drug delivery behavior of silica nanoparticles synthesized by P123-assisted sol-gel method. *Mater Chem Phys* 2018;205:283-91.
- Mehrafzoon S, Hassanzadeh-Tabrizi SA, Bigham A. Synthesis of nanoporous Baghdadite by a modified sol-gel method and its structural and controlled release properties. *Ceram Int* 2018;44:13951-8.
- Bigham A, Aghajanian AH, Allahdaneh S, Hassanzadeh-Tabrizi SA. Multifunctional mesoporous magnetic Mg<sub>2</sub>SiO<sub>4</sub>-CuFe<sub>2</sub>O<sub>4</sub> core-shell nanocomposite for simultaneous bone cancer therapy and regeneration. *Ceram Int* 2019;45:19481-8.
- Ansari A, Bigham A, Hassanzadeh-Tabrizi SA, Ahangar AH. Copper-substituted spinel Zn-Mg ferrite nanoparticles as potential heating agents for hyperthermia. *J Am Ceram Soc* 2018;101:3649-61.
- Yazdimamaghani M, Razavi M, Vashae D, Moharamzadeh K, Boccaccini AR, Tayebi L. Porous magnesium-based scaffolds for tissue engineering. *Mater Sci Eng C Mater*

Biol Appl 2017;71:1253-66.

22. Ansari M, Bigham A, Ahangar HA. Super-paramagnetic nanostructured CuZnMg mixed spinel ferrite for bone tissue regeneration. *Mater Sci Eng C Mater Biol Appl* 2019;105:110084.

23. Bigham A, Hassanzadeh-Tabrizi SA, Khamsehashari A, Chami A. Surfactant-assisted sol-gel synthesis and characterization of hierarchical nanoporous merwinite with controllable drug release. *J Sol Gel Sci Technol* 2018;87:618-25.

---

## BIOGRAPHIES



**Ashkan Bigham** received his M.Sc of Materials Science and Engineering from Islamic Azad University of Najafabad in 2016. Currently he is a research member of Prof. Mohammad Rafienia's group in the Department of Biomaterials of Isfahan University of Medical Sciences, Isfahan, Iran. His research interests focus on the

synthesis and application of bioceramics and biocomposites for bone tissue regeneration.

**Email:** ashkanbigham@gmail.com



**Saeed Kermani** obtained his B.Sc degree from the Department of Electrical Engineering of Isfahan University of Technology in Isfahan, Iran in 1987; he received the M.Sc degree in Bioelectric Engineering from Sharif University of Technology in 1992; he obtained his PhD in Bioelectric Engineering from Amirkabir

University of Technology, Tehran, Iran, in 2008. He is an Associate Professor of Bioelectrics and Biomedical Engineering in the Isfahan University of Medical Sciences, Iran. His research interests are in construction and operation of medical equipment, medical images, and signal processing.

**Email:** kermani@med.mui.ac.ir



**Ahmad Saudi** received the B.Sc degree in Biomechanics from Shiraz Payame Noor University, Shiraz, Iran, in 2016. After that, he obtained the M.S degree in biomaterials from Isfahan University of Medical Sciences, Isfahan, Iran, in 2019. His research interests focus on polymer & ceramic synthesis, nerve regeneration, and bone tissue engineering.

**Email:** ahmad.saudi2013@gmail.com



**Amir Hamed Aghajani** received the B.Sc degree in Materials Engineering from Najafabad Islamic Azad University, Najafabad, Iran, in 2013. After that, he obtained the M.Sc degree in Materials Engineering from Razi University, kermanshah, Iran, in 2018. His research interests focus on biomaterials, composite and bone tissue engineering.

**Email:** ahaghajaniyan67@gmail.com



**Mohammad Rafienia** obtained his B.Sc and both M.Sc and Ph.D. from Isfahan University of Technology and Amir Kabir University of Technology, respectively. He is currently the Professor of Biosensor Research Center of Isfahan University of Medical Sciences. His research expertise is in biomaterials, tissue engineering, and drug delivery.

**Email:** m\_rafienia@med.mui.ac.ir